

Ekaterina A. Khramtsova*, Alexandra A. Ageeva,
Alexander A. Stepanov, Viktor F. Plyusnin
and Tatyana V. Leshina

Photoinduced Electron Transfer in Dyads with (R)-/(S)-Naproxen and (S)-Tryptophan

DOI 10.1515/zpch-2016-0842

Received June 28, 2016; accepted September 19, 2016

Abstract: Short-lived intermediates arising from the donor-acceptor interaction of non-steroidal anti-inflammatory drug (NSAID) – (S)-naproxen (NPX) and its (R)-enantiomer with the tryptophan amino acid residue (Trp) have been studied by spin chemistry and photochemistry methods. The donor-acceptor interaction has carried out in a model linked system – dyad under the UV-irradiation. Interest in the NPX-Trp dyad diastereomers is connected with the possibility of using them as models of ligand-enzyme binding as long as amino acid residues are located at the enzyme's active centers. It is these residues that interact with NSAID during the binding. It is widely thought that charge transfer processes are involved in the process of drug-enzyme binding. Withing this framework the role of charge transfer in NPX-Trp excited state quenching have been investigated. The analysis of the chemically induced dynamic nuclear polarization (CIDNP), as well as fluorescence kinetics and quantum yield in different polarity media has shown that the main channel of NPX fluorescence quenching is the intramolecular electron transfer between NPX and Trp fragments. Electron transfer rate constants and fluorescence quantum yields of diastereomers have demonstrated stereodifferentiation.

Keywords: chirality; CIDNP; dyads; fluorescence spectroscopy; intramolecular electron transfer.

Dedicated to: Kev Salikhov on the occasion of his 80th birthday.

***Corresponding author: Ekaterina A. Khramtsova,** Voevodsky Institute of Chemical Kinetics and Combustion SB RAS, 630090, Institutskaya str. 3, Novosibirsk, Russia; and Novosibirsk State University, 630090, Pirogova str. 2, Novosibirsk, Russia, e-mail: khramtsovaea@gmail.com
Alexandra A. Ageeva, Alexander A. Stepanov and Tatyana V. Leshina: Voevodsky Institute of Chemical Kinetics and Combustion SB RAS, 630090, Institutskaya str. 3, Novosibirsk, Russia
Viktor F. Plyusnin: Voevodsky Institute of Chemical Kinetics and Combustion SB RAS, 630090, Institutskaya str. 3, Novosibirsk, Russia; and Novosibirsk State University, 630090, Pirogova str. 2, Novosibirsk, Russia

1 Introduction

Naproxen (NPX), particularly its stereoselectivity [differences in (R)- and (S)-isomers reactivity], is currently in scientific focus [1–5]. Interest in difference of (R)- and (S)-NPX optical isomers activity is due to their different therapeutic properties. Thus, its anti-inflammatory effect consists of cyclooxygenase (COX-1 and COX-2) enzyme inhibition, this effect is demonstrated by (S)-enantiomer only [1]. At the same time, it has been shown recently that both optical isomers inhibit the oxidation of cannabinoids [3] and prevent some types of cancer [6]. Intensive physicochemical and biochemical studies are carried simultaneously due to the finding of new therapeutic activities for both isomers of NPX and other well-known chiral non-steroidal anti-inflammatory drugs (NSAIDs) [2–4, 7].

Today the chemical nature of the differences in the enantiomers reactivity, including many examples in biological systems (therapeutic activity) is not established completely. The reason for the existence of such differences is that the enantiomers of drugs in living systems typically interact with other chiral compounds.

In recent times so-called linked systems (dyads) are increasingly used for the modeling of biomolecules interactions [8–10]. NPX and other NSAIDs enantiomers, as parts of linked systems – dyads, are the most extensively studied by using their photoinduced transformations [11–19]. It is believed that the photoinduced electron transfer and exciplex formation (partial charge transfer) can simulate the binding of NSAIDs with the COX's active sites [19]. In particular, it has been shown the significant differences in some photophysical properties of the dyads diastereomers, containing (R)- and (S)-NPX and (S)-N-methylpyrrolidine (NPX-Pyr), connected by various bridges, in different polarity media: the rate constants of the exciplex formation (state with partial charge transfer), exciplex fluorescence quantum yield [19]. Furthermore, it has been demonstrated some correlation between the exciplex fluorescence quantum yields and the efficiency of chemically induced dynamic nuclear polarization (CIDNP) detected in the act of a back electron transfer in NPX-Pyr dyads during their UV-irradiation. Thus, at present the stereoselectivity of charge transfer process in dyads comprising of (R)- and (S)-NPX can be considered as established. Therefore, obtained data indicate at the greater activity of the (R)-enantiomer in electron transfer process, while the (S)-enantiomer is more inclined to a reversible binding (formation of exciplex).

Considering that NPX in the active sites of COX-1 and COX-2 enzymes is bound with chiral amino acids residues, the study of charge transfer processes in dyads, including amino acids, sparks greater potential interest. Indeed, such research of (R,S)- and (S,S)-naproxen-tryptophan (NPX-Trp) dyads by using photochemistry methods (flash-photolysis, fluorescence spectroscopy) has been performed

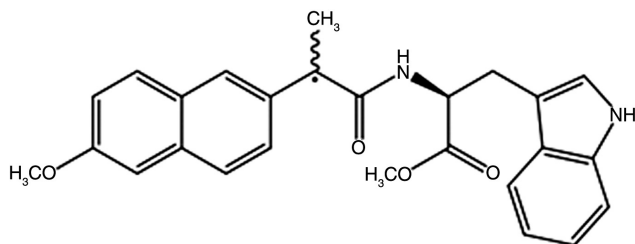


Chart 1: Chemical structure of dyad naproxen-tryptophan (NPX-Trp).

in the works of prof. M. Miranda et al. [14]. The results of these studies have been the registration of singlet energy transfer from tryptophan to naproxen moiety (Förster mechanism) and the assumption of exciplex formation under the UV-irradiation of NPX-Trp dyad diastereomers. Meanwhile, not only partial (exciplex formation) but full charge transfer (biradical-zwitterion formation) in this dyad is quite possible, according to Rehm-Weller criterion [16, 20].

This study is devoted to the proof-taking of the realization of partial and full charge transfer processes in the quenching of photoinduced excitation in (R,S)- and (S,S)- dyads, comprising of (R)-/(S)-NPX and (S)-tryptophan (Trp) (Chart 1).

Chemically induced dynamic nuclear polarization method (CIDNP) in high magnetic fields along with time-resolved fluorescence spectroscopy are used for the investigation of charge transfer processes in NPX-Trp diastereomers. It can be expected that the joined analysis of CIDNP and fluorescence data (in different polarity media) will allow to estimate the role of all short-lived intermediates in the process of photoexcitation quenching in (R,S)- and (S,S)-NPX-Trp dyads.

2 Experimental details

2.1 Synthesis of the substrates

The mixture of 2 mmol of (S)- or (R)-NPX in CH_2Cl_2 (4 mL) and 2 mmol of oxalyl chloride was maintained under stirring for 4 h. Then solvents were evaporated, also added 2 mmol methyl ether amino acid in dry toluene (8 mL) and Et_3N (0.5 mL) and the mixture was stirred for 22 h. The precipitate was filtered and washed with water. The crude product was recrystallized from toluene to afford (S,S)- or (R,S)-NPX-Trp (0.71 g, 71%), m.p. 156–158 °C. ^1H NMR (CDCl_3) δ : 7.77 (br.s 1H), 7.75–7.70 (m, 3H), 7.41–7.39 (dd, $J_1=8.4$ Hz, $J_2=1.8$ Hz, 1H), 7.18–7.12 (m, 2H), 5.89 (m, 1H), 4.06–3.88 (m, 2H), 3.92 (s, 3H), 3.77 (q, 1H, $J=7.2$ Hz), 3.70 (s, 3H),

1.62 (d, 3H, $J = 7.2$ Hz). ^{13}C NMR (CDCl_3) δ : 174.0, 172.2, 157.7, 135.9, 135.8, 133.7, 129.3, 128.9, 127.43, 127.42, 126.4, 126.1, 122.5, 122.1, 119.6, 119.0, 118.4, 111.1, 109.7, 105.6, 55.3, 52.7, 52.2, 46.9, 27.2, 18.1. Anal. Calcd for $\text{C}_{26}\text{H}_{26}\text{N}_2\text{O}_4$: C 72.54; H 6.09; N 6.51. Found: C 72.64; H 6.03; N 6.51.

2.2 Preparation of solutions

Stock solutions were prepared in two solvents: acetonitrile (Cryochrom, $\epsilon = 36.8$) [21] or benzene (Soyuzchemprom, $\epsilon = 2.28$) [22] for optic measurements and deuterioacetonitrile (D 99.9%) and deuterobenzene (D 99.8%), both by Aldrich, for CIDNP measurements. Solvent permittivity values are shown for 293 K. The solvent permittivities for the mixtures were taken from the literature [23]. There is no room for doubt that the linear correlation between solvent polarity and its dielectric coefficient, and so we use both term hereafter. Concentrations of dyads in stock solutions for optic measurements were kept about 1.0×10^{-4} M or 5.0×10^{-3} M for CIDNP experiments to exclude all potential bimolecular reactions.

2.3 CIDNP measurements

^1H pseudo steady state (PSS) [24] and time-resolved (TR) CIDNP experiments were performed on DPX-200 NMR spectrometer (Bruker, 200 MHz ^1H operating frequency, $\tau(90) = 3.0 \mu\text{s}$ with using preamplifier). In all experiments the first step was the non-selective presaturation procedure. After that in TR-experiments the next sequence follows: the laser pulse (~ 15 ns), variable time delay ($0 \mu\text{s}$ in our case), radio-frequency (RF) registration pulse ($2\text{--}4 \mu\text{s}$). In PSS-experiments: time delay 2.56 s (needs to be less than the characteristic relaxation time of nuclei), 180° – RF pulse, 32 laser pulses (total duration 2.56 s), RF-registration pulse.

The samples in standard 5 mm Pyrex NMR tubes were irradiated directly in the probe of the NMR spectrometer. EMG 101 MSC excimer laser was used as a light source (Lambda Physik, 308 nm, 100 mJ at output window, 20 mJ per pulse in sample volume, with pulse duration 15 ns). The samples were deoxygenized by bubbling argon for 15 min just before irradiation.

2.4 Fluorescence measurements

All spectroscopic measurements were performed using a quartz cuvette of 1 cm optical length. Spectra and kinetic curves of luminescence were recorded with an

Edinburgh Instruments FLSP-920 spectrofluorometer with either a Xenon lamp or a laser diode EPLED-320 ($\lambda_{\text{ex}} = 320$ nm, pulse duration 0.6 ns) as excitation sources. The kinetic traces were fitted by exponential decay functions using a reconvolution procedure.

Luminescence quantum yields were measured relative to that of NPX, using the value for the fluorescence quantum yield of naproxen in acetonitrile (0.47, [25]), as it has been previously shown that quantum yield of naproxen fluorescence is basically solvent-independent. All samples were bubbled with argon for 30 min to remove dissolved oxygen just before the experiments. After every experimental series a control fluorescence spectrum was recorded for checking the absence of oxygen in samples. All experiments were performed at room temperature 296 K.

2.5 Optic measurements

The absorbance at the excitation wavelength was kept ca. 0.1. UV/Visible absorption spectra were recorded using an Agilent 8453 spectrophotometer (Agilent Technologies). Extinction coefficients have been obtained for the estimation of NPX vs. Trp moieties absorption fractions at the different experimental conditions: in fluorescence experiments $\epsilon_{\lambda=300 \text{ nm}} = 1150 \pm 20 \text{ M}^{-1} \text{ cm}^{-1}$, in CIDNP – $\epsilon_{\lambda=308 \text{ nm}} = 850 \pm 10 \text{ M}^{-1} \text{ cm}^{-1}$ for both diastereoisomers.

3 Results and discussion

To confirm the hypothesis about the possibility of electron transfer between the (R)- and (S)-NPX and acetyl (S)- tryptophan, we have used the ¹H-CIDNP effects, arising under the UV-irradiation of the NPX-Trp dyad in the solutions with different dielectric constants (Figure 1).

Joined analysis of spectra pictured in Figure 1 let us identify the following polarized protons: the aromatic protons at the position 4' (or 8') and 5' of NPX fragment show negative polarization as well as the protons of methylene group of the tryptophan residue. At the same time, protons at the position 2, 4(7), 6 of indole ring show positive polarization. The signals, situated in the area of the resonance of methyl group and belonged to a chiral center, also demonstrate chemical polarization but the contribution of these CIDNP effects is very different for TR- and PSS-spectra.

The additional signals of methyl proton have been also found in small quantities in the stationary NMR spectrum, detected after the UV-irradiation of NPX-Trp

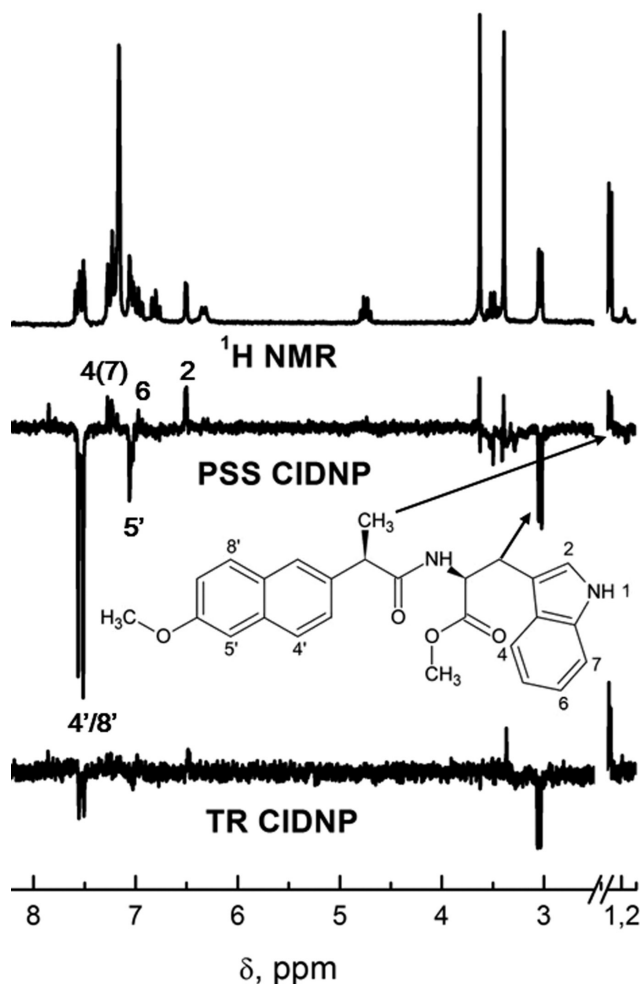


Fig. 1: ^1H NMR of 5 mM (R,S)-NPX-Trp in 40% deuterioacetonitrile- 60% deuterobenzene mixture (top), PSS- (dark spectrum is subtracted, middle) and TR-CIDNP (bottom) spectra.

dyads (Figure 2). Obviously, these signals are referred to the parallel radical process of minor NPX-Trp dyads photodegradation. Mark that the same polarized signals have been observed in NPX photolysis, that is known to undergo a partial photodegradation via decarboxylation [26]. The preferential presence of signals belonged to the methyl group in TR-spectrum points at they form in the minor cage process.

Since it was previously suggested that one of the ways of the dyad's excited state quenching was electron transfer, one should expect that the main process

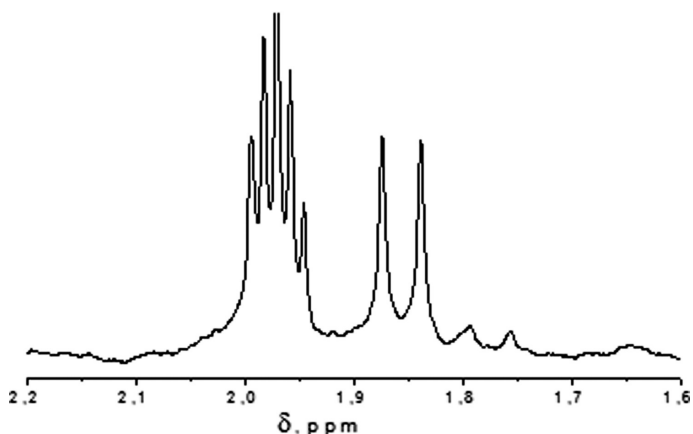


Fig. 2: Fragment of the ^1H NMR spectrum of (S,S)-NPX-Trp after photolysis in 40% deuterioacetone-nitrile- 60% deuterobenzene mixture. Doublet situated at 1.77 ppm belong to methyl protons of one of the photodegradation products.

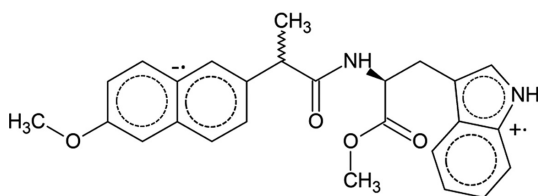
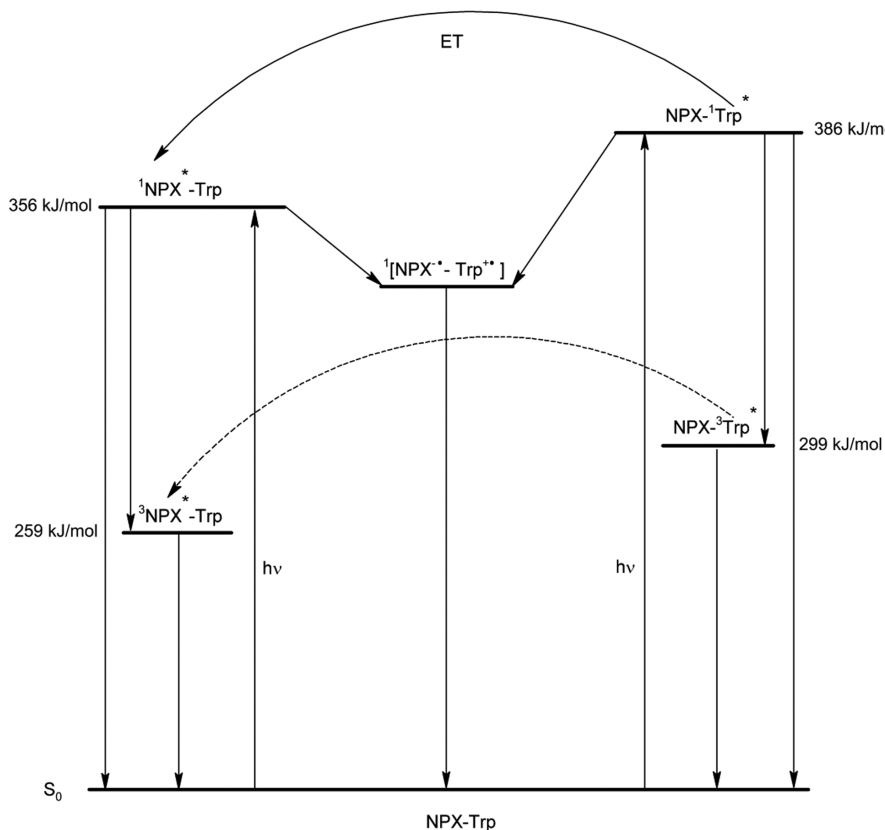


Fig. 3: Biradical-zwitterion (BZ) NPX-Trp.

is the formation of the corresponding biradical-zwitterion (BZ), where a negative charge is concentrated at NPX fragment and positive at Trp (Figure 3) [14].

According to the Scheme 1, BZ is obtained as a result of the quenching of the NPX chromophore singlet excited state by Trp. Note, that the same BZ would be formed if NPX, in its ground state, was the quencher of Trp singlet excited state; but at these experimental conditions the light is predominantly absorbed by NPX itself (97%).

It should be also emphasized that the basic contribution is the intramolecular ET, since the rate constant of the dyad's singlet excited state quenching ($6\text{--}8 \cdot 10^8 \text{ s}^{-1}$) is for an order higher than the possible rate of bimolecular process ($W = 2 \cdot 10^9 \cdot 5 \cdot 10^{-3} = 10^7 \text{ M}^{-1} \cdot \text{s}^{-1}$). But the considerable rise of CIDNP intensity of the NPX and Trp main lines in PSS-spectrum versus TR-analog points at the contribution of bimolecular ET – the quenching of the dyad in the excited singlet state by its ground state. Note that the CIDNP effects are identical in both ET processes.



Scheme 1: Photoinduced processes in NPX-Trp dyad.

With that, CIDNP in the dyads, containing NPX, studied earlier were described by $S-T_0$ approximation, although the appearance of electron exchange interaction had been demonstrated for one of the dyads [18]. However, the presence of the CIDNP effects with different signs in the NPX-Trp dyads directly indicates at the $S-T_0$ -mechanism manifestation. It can be suggested that in this case the energy of electron exchange interaction influence CIDNP intensity only because spin evolution progresses out of the $S-T_+$ -crossing area, majorly [18]. The similarity of TR- and PSS-CIDNP effects confirms this suggestion.

CIDNP signs analysis has been carried out by using Kaptein rules for high magnetic fields, modified by Closs, which takes into account the possibility of the recombination of the radical pair triplet state of [27]. It is necessary since there is the possibility of a recombination from both spin states of BZ. Taking into account that: the g-factor of NPX is higher than those of Trp [28–30], HFI constants for the aromatic

and indole protons are negative for methylene – positive [30–32]; it turns out that if electron transfer occurs, it takes place between $^1\text{NPX}^*$ and Trp in its ground state. At that, back ET would occur mainly from ^3BZ . By the way, the process of diffusion quenching of naphthalene by triethylamine demonstrates the recombination constant from the T spin state of ion-radical pairs higher than from the S [33].

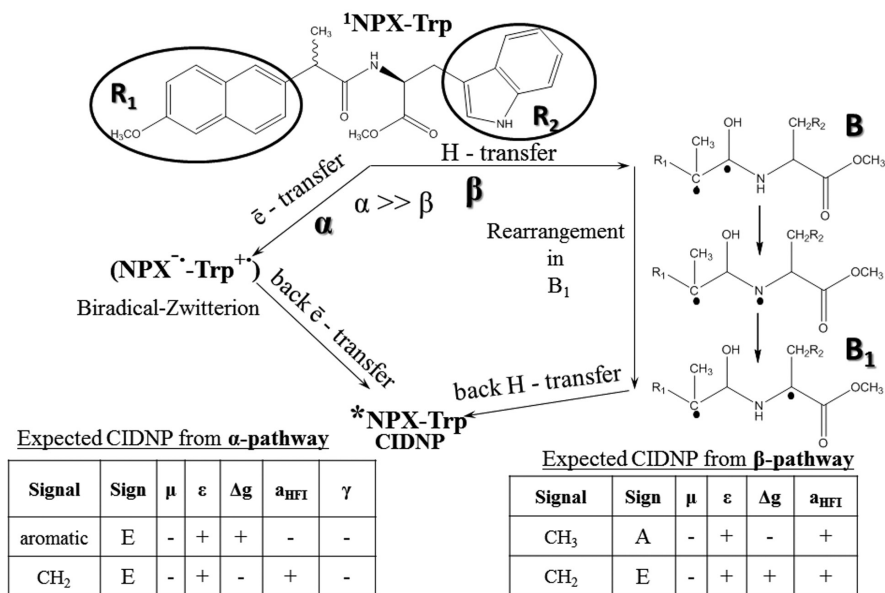
Thus, the analysis of the CIDNP effects confirms the reversible electron transfer in the NPX-Trp dyad. For additional verification of processes contribution to the CIDNP, we have compared the CIDNP effectivity ratios of different protons in (R,S)-NPX-Trp dyad with the ratios of corresponding HFI constants. The HFI constants ratios of NPX aromatic protons at $8'$ position and CH_2 -group of Trp are: 0.495 mT and 0.7–1.0 mT = 1.0; 1.7. These average ratios in TR-spectra are 1.0; 1.66. Thus, the ratio of NPX and β - CH_2 -protons corresponds to the spin density distribution in BZ.

However, the appearance of polarized signals in the region of the NPX methyl protons resonance indicates at the existence of a one more reversible process – the H atom transfer from the NPX's chiral center. The absence of CIDNP effect at the CH-group itself points at the small HFI constant of this proton in radical-partner – the carbonyl group of Trp, presumably (see Scheme 2). According to Kaptein rule the CIDNP can be created in neutral biradical B_1 (β -way) in singlet spin state, which, in turn, obtained from the dyad's singlet excited state. Biradical B_1 is obtained as a result of successive rearrangements – a free valence migration that is typical for paramagnetic particles from amino acids [34].

Apparently, the TR-spectrum (Figure 1) is the combination of CIDNP effects formed in BZ and B_1 (see Scheme 2). At the same time, PSS-spectrum contains all the lines that have to be polarized in the back ET stage and only the small fraction of polarized methyl protons from the neutral biradical B_1 . It points at B_1 is really biradical, which can not be obtained via the bimolecular quenching of $^1\text{NPX-Trp}$.

Furthermore, the shape of the CIDNP dependence on the solvent polarity points at the existence of two parallel processes of dyad's phototransformation. The obtained CIDNP dependence is shown in Figure 4.

In discussing these dependences it should be taken into account that CIDNP in the linked systems is determined not only by HFI values and g -factors differences but the distance between radical centers, that plays decisive role [35–37]. The CIDNP dependence on solvent polarity reflects the alternation in BZ energy level positions in the media with different dielectric constants. Wherein the BZ lifetime can change as well as the recombination constants. In the system under study the decrease of CIDNP effectivity in strong polarity media (CH_3CN) is the most probable the result of k_s and k_t values rapprochement [16, 19]. In the same time, the CIDNP of methyl protons in the chiral center does not practically depend on solvent polarity (Figure 4). This is an additional confirmation of this CIDNP creation in neutral biradical (Scheme 2).



Scheme 2: Phototransformation of NPX-Trp dyad and CIDNP analysis.

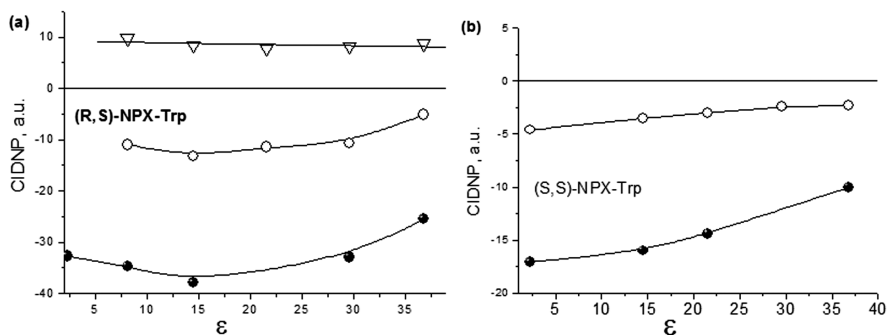


Fig. 4: CIDNP effectivity dependence on solvent polarity of CH₂-protons (Trp, ◯) and aromatic protons (NPX, ●) for (R,S)-NPX-Trp (a) and (S,S)-NPX-Trp (b); CH₃-protons (NPX, ▽) for (R,S)-NPX-Trp in deuteroacetonitrile-deutero benzene mixtures.

Consequently, the CIDNP analysis allows to highlight four processes, carried out in the system under study under the UV-irradiation. They are an intramolecular electron transfer and its bimolecular analog, H atom transfer with a partial degradation of a dyad. Both ET demonstrate identical CIDNP effects. All effects are described by a pair, where a positive charge is located at the Trp-part and a

negative – at NPX part. The partial degradation maintains through the C–C(O) bond breaking, presumably.

Besides that the shapes of the CIDNP effectivity dependence for NPX and Trp protons on dielectric constant differ greatly from those measured earlier for their analogs: dyads “naproxen – N methyl pyrrolidine”, where the CIDNP reflects a rapid dynamic equilibrium between BZ and exciplex [15, 16, 19]. In that cases there are curves with a maximum in the area of weak polarity ($\epsilon=6-12$), where, according to Rehm–Weller criterion [20], exciplex should appear. As it can be seen from Figure 2, the CIDNP effectivity dependence on the solvent polarity for dyad NPX-Trp are significantly less pronounced and has no maximum in the abovementioned area for the both diastereomers.

Another attempt to find exciplex in the photolysis of the NPX-Trp diastereomers has been fluorescence spectroscopy application. The fluorescence spectra of dyads diastereomers, AcTrp and MeNPX are presented below (Figure 5).

Fluorescence spectra of dyads are similar to MeNPX with the maximum at 350 nm, however, they are far less intensive. Furthermore, fluorescence from Trp moiety has not been registered (AcTrp fluorescence spectrum has maximum at 330 nm, fluorescence quantum yield 0.16 in acetonitrile). The absence of tryptophan fluorescence, according to the reference data [14], is explained by the singlet energy transfer from $^1\text{Trp}^*$ to the NPX by Förster mechanism.

It should be noted, that, unlike previously studied dyads comprising NPX, for NPX-Trp dyads the formation of exciplex during UV-irradiation has not been found (Figure 5).

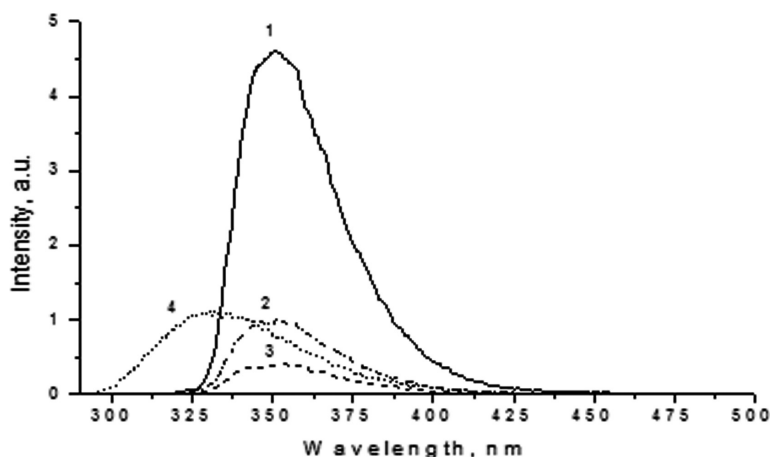


Fig. 5: Fluorescence spectra ($\lambda_{\text{ex}}=300$ nm) for MeNPX (1) and dyads (S,S)- (2) and (R,S)- (3) NPX-Trp in benzene; ($\lambda_{\text{ex}}=280$ nm) N-AcTrp (4) in acetonitrile. All concentrations $\sim 10^{-4}$ M.

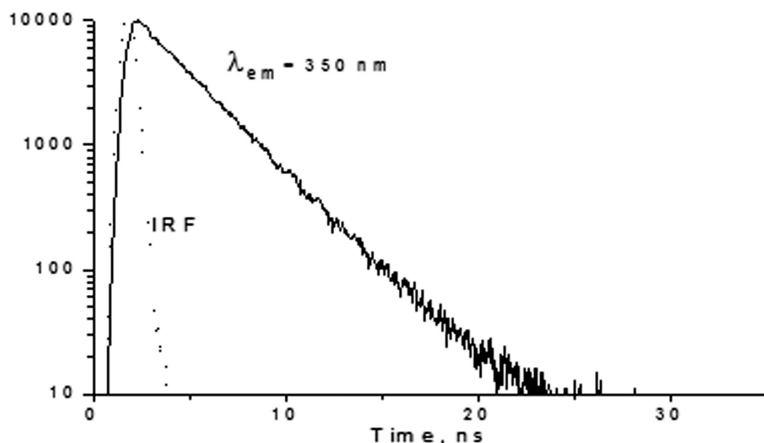


Fig. 6: Fluorescence decay of (S,S)-NPX-Trp ($\lambda_{ex} = 300$ nm) in acetonitrile.

Fluorescence quantum yields have been obtained at the different polarity media by using usual technique [38]. Also, time-resolved experiments have been carried out at the different polarity media. Typical kinetic curve for (S,S)-NPX-Trp in acetonitrile is shown in Figure 6.

These kinetics are described by monoexponential function. As a result, fluorescence lifetimes have been obtained for both diastereomers. So, for dyads (S,S)-NPX-Trp and (R,S)-NPX-Trp, there is more efficient fluorescence quenching than for free naproxen ($\phi = 0.47$ [25]), indicating at the appearance of additional quenching channels. However, this channel is not the exciplex formation, as it has been supposed in the work [14]. Meanwhile, as well as the abovementioned other dyads, NPX-Trp diastereomers demonstrate the difference in fluorescence quantum yield and lifetimes (Table 1).

The stereodifferentiation in this system has also been observed earlier in the work [14], where exciplex has been considered as a source of it. Considering about the mechanisms of NPX excitation quenching in the dyad NPX-Trp and the nature of this process stereoselectivity, the following circumstances must be taken into account. There are reference data about the observation of triplet excited state in NPX-Trp dyads, obtained by the flash-photolysis: triplet quantum yield of $^3\text{NPX}^*\text{-Trp}$ is much less than for $^3\text{NPX}^*$ ($\phi_T = 0.28$) [14]. It has been explained by the effective quenching of $^1\text{NPX}^*$ by Trp. All experimental data, presented in the literature and our own (a miserable fluorescence quantum yield of the NPX local excited state, a small triplet quantum yield of the NPX-Trp dyad, the lack of Trp fluorescence) lead to the conclusion that these results can not be explained only by energy transfer from Trp to NPX.

Tab. 1: Fluorescence lifetimes (τ_{fl}), quantum yields (ϕ_{fl}) and electron transfer rate constants (k_{ET}) in the different polarity media (acetonitrile-benzene mixture).

ϵ	(R,S)-NPX-Trp			(S,S)-NPX-Trp		
	τ_{fl} , ns	ϕ_{fl}	$k_{ET} \cdot 10^{-8} \text{ s}^{-1}$	τ_{fl} , ns	ϕ_{fl}	$k_{ET} \cdot 10^{-8} \text{ s}^{-1}$
36.8	1.2 ± 0.1	0.036 ± 0.005	8.0 ± 0.1	2.9 ± 0.3	0.11 ± 0.02	3.1 ± 0.3
29.6	1.2 ± 0.1	0.038 ± 0.006	8.0 ± 0.1	2.9 ± 0.3	0.11 ± 0.02	3.1 ± 0.3
21.55	1.3 ± 0.1	0.051 ± 0.008	7.3 ± 0.1	3.0 ± 0.3	0.12 ± 0.02	2.9 ± 0.3
16.1	1.4 ± 0.1	0.053 ± 0.008	6.7 ± 0.1	3.0 ± 0.3	0.13 ± 0.02	2.9 ± 0.3
8.08	1.5 ± 0.2	0.057 ± 0.009	6.3 ± 0.2	3.0 ± 0.3	0.13 ± 0.02	2.9 ± 0.3
2.28	1.5 ± 0.2	0.067 ± 0.01	6.2 ± 0.2	2.7 ± 0.3	0.13 ± 0.02	3.2 ± 0.3

It is reasonable to assume that the quenching of the chromophores excited states takes place through several channels. So, the quenching of ${}^1\text{NPX}^*\text{-Trp}$ involves electron transfer, as indicates the CIDNP effects. On the other side, the quenching of $\text{NPX}^*\text{-Trp}^*$ can also occur *via* electron transfer to NPX-Trp in its ground state. ${}^1\text{Trp}^*$ quenching by NPX also involves an energy transfer. We have attempted to summarize all the photoinitiated processes, which may take place between NPX and Trp, in the scheme (see Scheme 1).

According to this scheme the small magnitude of fluorescence quantum yields of both chromophores (NPX and Trp), and triplet quantum yields can be explained by assuming that the energy transfer follows by fast (in the same time range) electron transfer that, on its turn, lead to the fluorescence quenching. Indeed, the rate constants, listed in Table 1, are more than an order of magnitude higher than those for dyads “naproxen -pyrrolidine” [17, 19].

Thus, the electron transfer in dyads containing naproxen and an amino acid residue – tryptophan can be regarded as the established main process of chromophores excitation quenching.

Acknowledgments: The work was supported by the Russian Foundation for Fundamental Research (14-03-00192, 14-03-00692). The authors also are very grateful to P.A. Purtov and A.I. Kruppa for helpful discussions.

References

1. A. M. Evans, *Eur. J. Clin. Pharmacol.* **42** (1992) 237.
2. K. C. Duggan, M. J. Walters, J. Musee, J. M. Harp, J. R. Kiefer, J. A. Oaters, L. J. Marnett, *J. Biol. Chem.* **285** (2010) 34950.

3. K. C. Duggan, D. J. Hermanson, J. Musee, J. J. Prusakiewicz, J. L. Scheib, B. D. Carter, S. Banerjee, J. A. Oaters, L. J. Marnett, *Nature Chem. Biol.* **7** (2011) 803.
4. Q. Shen, L. Wang, H. Zhou, H. Jiang, L. Yu, S. Zeng, *Acta Pharmacol. Sinica* **34** (2013) 998.
5. M. Gonzalez-Bejar, E. Alarcon, H. Poblete, J. C. Scaiano, J. Perez-Prieto, *Biomacromolecules* **11** (2010) 2255.
6. M.-S. Kim, J.-E. Kim, D. Y. Lim, Z. Huang, H. Chen, A. Langfald, R. A. Lubet, C. J. Grubbs, Z. Dong, A. M. Bodel, *J. Cancer Prev.* **7** (2014) 236.
7. I. Vaya, V. Lhiaubet-Vallet, M. C. Jimenez, M. A. Miranda, *Chem. Soc. Rev.* **43** (2014) 4102.
8. V. Balzani, M. Venturi, A. Credi, *Molecular Devices and Machines: A Journey into the Nanoworld*, John Wiley & Sons, Germany (2006).
9. K. Möbius, A. Savitsky, *High-field EPR Spectroscopy on Proteins and Their Model Systems: Characterization of Transient Paramagnetic States*, RSC, USA (2009).
10. K. Ohkubo, S. Fukuzumi, *Bull. Chem. Soc. Jpn.* **82** (2009) 303.
11. V. Lhiaubet-Vallet, F. Bosca, M. A. Miranda, *J. Phys. Chem. B* **111** (2007) 423.
12. I. Vaya, M. C. Jimenez, M. A. Miranda, *J. Phys. Chem. B* **111** (2007) 9363.
13. P. Bonancia, I. Vaya, M. J. Climent, T. Gustavsson, D. Markovitsi, M. C. Jimenez, M. A. Miranda, *J. Phys. Chem. A* **116** (2012) 8807.
14. I. Vaya, I. Andreu, M. C. Jimenez, M. A. Miranda, *Photochem. Photobiol. Sci.* **13** (2014) 224.
15. I. M. Magin, N. E. Polyakov, E. A. Khramtsova, A. I. Kruppa, Yu. P. Tsentlovich, T. V. Leshina, M. A. Miranda, E. Nuin, M. L. Marin, *Chem. Phys. Lett.* **516** (2011) 51.
16. I. M. Magin, N. E. Polyakov, E. A. Khramtsova, A. I. Kruppa, A. A. Stepanov, P. A. Purtov, T. V. Leshina, Yu. P. Tsentlovich, M. A. Miranda, E. Nuin, M. L. Marin, *Appl. Magn. Reson.* **41** (2011) 205.
17. E. A. Khramtsova, V. F. Plyusnin, I. M. Magin, A. I. Kruppa, N. E. Polyakov, T. V. Leshina, E. Nuin, M. L. Marin, M. A. Miranda, *J. Phys. Chem. B* **117** (2013) 16206.
18. I. M. Magin, N. E. Polyakov, A. I. Kruppa, P. A. Purtov, T. V. Leshina, A. S. Kiryutin, M. A. Miranda, E. Nuin, M. L. Marin, *Phys. Chem. Chem. Phys.* **18** (2016) 901.
19. E. A. Khramtsova, D. V. Sosnovsky, A. A. Ageeva, E. Nuin, M. L. Marin, P. A. Purtov, S. S. Borisevich, S. L. Khursan, H. D. Roth, M. A. Miranda, V. F. Plyusnin, T. V. Leshina, *Phys. Chem. Chem. Phys.* **18** (2016) 12733.
20. D. Rehm, A. Weller, *Bunsen-Ges. Phys. Chem.* **73** (1969) 834.
21. G. P. Cunningham, J. A. Vidulich, R. L. Kay, *J. Chem. Eng. Data* **12** (1967) 336.
22. A. A. Mariott, E. R. Smith, *Table of Dielectric Constants of Pure Liquids*, NBS, USA (1951).
23. Y. Y. Ahadov, *Dielektrichiskie svoystva binarnich rastvorov*, Nauka, Russia (1977).
24. M. Goetz, *Chem. Phys. Lett.* **188** (1992) 451.
25. U. Pischel, S. Abad, M. A. Miranda, *Chem. Comm.* **9** (2003) 1088.
26. F. Bosca, M. A. Miranda, L. Vano, F. Vargas, *J. Photochem. Photobiol. A* **54** (1990) 131.
27. G. L. Closs, M. S. Czeropski, *J. Am. Chem. Soc.* **99** (1977) 6127.
28. W. Schwarz, K.-M. Dangel, G. Jones II, J. Bargon, *J. Am. Chem. Soc.* **104** (1982) 5686.
29. N. N. Saprygina, O. B. Morozova, N. P. Gritsan, O. S. Fedorova, A. V. Yurkovskaya, *Russ. Chem. Bull., Int. Ed.* **60** (2011) 2529.
30. M. Wegner, H. Fischer, M. Koeberg, J. W. Verhoeven, A. M. Oliver, M. N. Paddon-Row, *Chem. Phys.* **242** (1999) 227.
31. N. S. Landolt-Bornstein, *Numerical Data and Functional Relationship in Science and Technology: Magnetic Properties of Free Radicals*, Springer-Verlag, Berlin (1988).
32. S. E. Walden, R. A. Wheeler, *J. Phys. Chem.* **100** (1996) 1530.

33. M. E. Michel-Beyerle, R. Haberkorn, W. Bube, E. Steffens, H. Schroeder, H. J. Neusser, E. W. Schlag, *Chem. Phys.* **17** (1976) 139.
34. M. Bonifacic, D. Armstrong, I. Carmichael, K. Asmus, *J. Phys. Chem. B* **104** (2000) 643.
35. J. Bargon, *J. Am. Chem. Soc.* **99** (1977) 8350.
36. E. Schaffner, H. Fischer, *J. Phys. Chem.* **100** (1996) 1657.
37. U. Wegner, H. Staerk, *J. Phys. Chem.* **99** (1995) 248.
38. D. F. Eaton, *Pure Appl. Chem.* **60** (1988) 1107.